JGP Journal of General Physiology

COMMENTARY

Zn^{2+} to probe voltage-gated proton (Hv1) channels

H. Peter Larsson

Voltage-gated proton (Hv1) channels are membrane proteins that conduct protons to remove acidic load inside cells (DeCoursey, 2013). They are also involved in the respiratory burst in leukocytes, important for the capacitation (activation) of sperm cells, and even generate the up stroke of action potentials (like voltage-gated Na^+ channels in neurons) in some dinoflagellates (DeCoursey, 2013). Hv1 channels are closed at physiological pH and resting potentials but activated by depolarizations and/or by intracellular acidification (DeCoursey, 2013). Hv1 channels are homologous to voltage-gated cation channels, such as voltage-gated K^+ (Kv), Na^+ (NaV), and Ca^{2+} (CaV) channels (Ramsey et al., 2006; Sasaki et al., 2006). Kv, NaV, and CaV channels are tetrameric channels (or have four homologous domains) with six transmembrane (TM) segments per subunit (or domain): the first four TM segments form a voltage-sensing domain, and the last two TM segments from all four subunits (or domains) together form the ion-conducting pore (Fig. 1 A; Long et al., 2005). In contrast, Hv1 channels are dimeric channels with only four transmembrane segments per subunit (Koch et al., 2008; Lee et al., 2008; Tombola et al., 2008), homologous to the voltage-sensing domain of other voltage-gated cation channels (Fig. 1 B). It is clear that each subunit of Hv1 channels contains its own proton permeation pathway (Fig. 1 B; Koch et al., 2008; Tombola et al., 2008), but how this pathway opens and closes in response to voltage is still not clear. The work from Cherny et al. (2020) in this issue provides more constraints on the closed and open states of Hv 1 channels.

Cysteine and histidine accessibility experiments (Gonzalez et al., 2010, 2013; Kulleperuma et al., 2013; Morgan et al., 2013), structures of the homologous voltage-sensing phosphatase (VSP) in different states (Li et al., 2014), a crystal structure of a Hv1-VSP chimera (Takeshita et al., 2014), EPR measurements on Hv1 (Li et al., 2015), and numerous mutagenesis studies and molecular simulations of Hv1 channels have generated different proposed models of Hv1 closed and open states (excellent review in Randolph et al., 2016; Fig. 2). Despite obvious differences between the proposed models, all of these models have in common the fact that the fourth TM segment, S4, is the main voltage sensor of Hv1: at hyperpolarized voltages S4 is in a retracted, inward state, but in response to depolarizations S4 moves outwards across the membrane and triggers channel opening. But how far S4 moves between the resting and activated state, what constitutes the actual gate, and how does the gate open in response to depolarizations are still questions that are hotly debated. Cherny and coworkers here use Zn^{2+} binding to WT and mutated Hv1 channels as a tool to further probe the closed and open states of Hv1, and especially the possible different states of S4 relative to the other TM segments in an Hv1 subunit (Cherny et al., 2020).

Zn^{2+} is a classical inhibitor of Hv1 channels (DeCoursey, 2013) and a physiologically important regulator of Hv1 activity in sperm: high extracellular Zn^{2+} concentrations in the semen keep Hv1 channels inhibited. However, the low extracellular Zn^{2+} concentrations in the vaginal tract increases Hv1 channel activation, which triggers a cascade that leads to turning on the beating of the sperm tail (Lishko et al., 2010). Zn^{2+} is thought to be mainly coordinated in mammalian Hv1 channels by two extracellularly located His residues: H140 in the S1-S2 loop and H193 in the S3-S4 loops (Fig. 1 B; Ramsey et al., 2006; Sasaki et al., 2006). Removing these two His residues almost completely eliminates the Zn^{2+} inhibition in mammalian Hv1 channels (Ramsey et al., 2006). However, other residues have also been implicated in Zn^{2+} binding (De La Rosa et al., 2018; Qiu et al., 2016; Takeshita et al., 2014). DeCoursey and coworkers here find that, in an Hv1 channel with the two native His residues removed (H140A/H193A), introducing a His in S1 at position V116 generates an Hv1 channel with extremely high Zn^{2+} affinity (Cherny et al., 2020). This affinity is too high for just a single His residue, so they searched for a residue that coordinates Zn^{2+} together with V116H. Mutations of an aspartate in S3, D185, was found to reduce the affinity dramatically in V116H Hv1 channels, as if Zn^{2+} is coordinated between V116H and D185. The homologous residue to D185 has previously been implicated in Zn^{2+} binding in mutant hHv1 (De La Rosa et al., 2018) and to the closed state of sea squirt Hv1 channels in earlier studies (Qiu et al., 2016). Thus, this residue might be involved in Zn^{2+} binding in WT Hv1 channels as well.

Next, the authors set out to determine how Zn^{2+} inhibits Hv1 channels. For this the authors cleverly turn to monomeric Hv1

Department of Physiology and Biophysics, University of Miami Miller School of Medicine, Miami, FL.

Correspondence to H. Peter Larsson: plarsson@med.miami.edu.

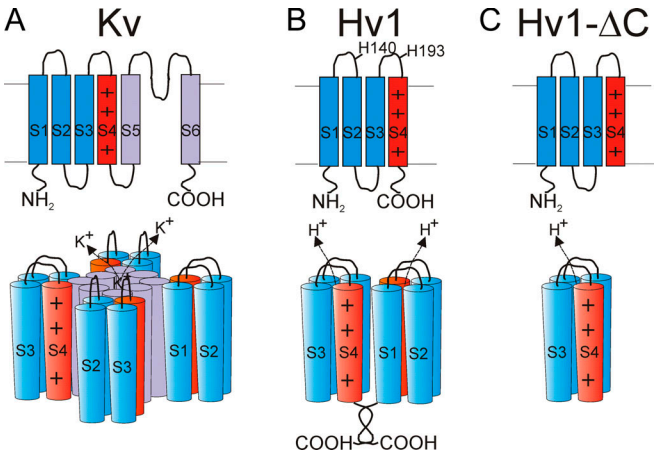

Figure 1. **Topology and subunit arrangements in different voltage-gated ion channels. (A)** Topology (top) and arrangement of the four subunits (bottom) of Kv channels with a central, common pore (made up of the four S5-S6 pore domains, one from each subunit) and four separate voltage-sensing domains (made up of S1-S4 in each subunit; Long et al., 2005). K^+ flows through the common central pore. A similar topology and arrangement are for NaV and CaV, but the four subunits are covalently linked into one long polypeptide with four six-TM domains. **(B)** Topology (top) and arrangement of the two subunits (bottom) of Hv1 channels (Ramsey et al., 2006; Sasaki et al., 2006). The two Hv1 subunits are held together by the coiled-coil formed by the two C termini (Li et al., 2010). Each subunit has its own H^+ conduction pathway (Koch et al., 2008; Tombola et al., 2008). His140 and His193 that coordinate Zn^{2+} in WT Hv1 channels are labeled. **(C)** Deletion of the C termini (Hv1-ΔC) separates the subunits into fully functional, monomeric Hv1 channels (Koch et al., 2008; Tombola et al., 2008).

channels. Normally, the two C termini of the two Hv1 subunits form a coiled-coil domain that keeps the two Hv1 subunits together (Fig. 1 B; Li et al., 2010). However, a dimeric Hv1 channel can be turned into two monomeric voltage-gated proton channels by removal of the two C termini (Fig. 1 C; Koch et al., 2008; Tombola et al., 2008). These monomeric channels are still voltage-gated proton channels and function similar to the WT dimeric Hv1 channels, but open much faster than the WT Hv1 channels (Koch et al., 2008; Tombola et al., 2008). Using these fast activating, monomeric versions of Hv1 channels, the authors find that Zn^{2+} binds with extremely high affinity (low nanomolar range) to the closed state of Hv1, but apparently not at all to the open state. Surprisingly, the kinetics of Hv1 V116H channel opening in the presence of Zn^{2+} is voltage independent, whereas the kinetics of opening for WT Hv1 channels in the presence and absence of Zn^{2+} and for monomeric Hv1 V116H in the absence of Zn^{2+} is clearly voltage dependent. The authors came up with a clever model to explain this, in which Zn^{2+} binding to the closed state prevents opening, and that Zn^{2+} has to unbind before the channel can open (Fig. 2, A and B). Due to the very fast opening kinetics of the monomeric Hv1 V116H channels, the rate-limiting step during activation in the presence of Zn^{2+} is therefore the relatively slow, voltage-independent unbinding of Zn^{2+}. In WT Hv1 channels, opening kinetics is still voltage dependent in the presence of Zn^{2+}, as if the mechanism of Zn^{2+} inhibition is different in WT and Hv1 V116H monomeric channels. However, this is just an apparent difference caused by the much slower opening kinetics in WT Hv1 channels. In WT Hv1 channels, the slow opening kinetics make the opening step the rate-limiting step and, therefore, Zn^{2+} unbinding is not rate limiting in WT Hv1 channels. Most likely, a similar general mechanism of Zn^{2+} inhibition occurs in WT and monomeric V116H channels (although obviously with different molecular binding sites: H140 and H193 in WT and V116H and D185 in V116H Hv1 channels): Zn^{2+} binding to the closed state prevents opening, and unbinding of Zn^{2+} is necessary for channel opening.

The most exciting finding of this paper is the additional structural constraints that these data generate for the models of the closed and open states of Hv1 channels. Even with all the data we have at this point—the crystal structures of Hv1-VSP

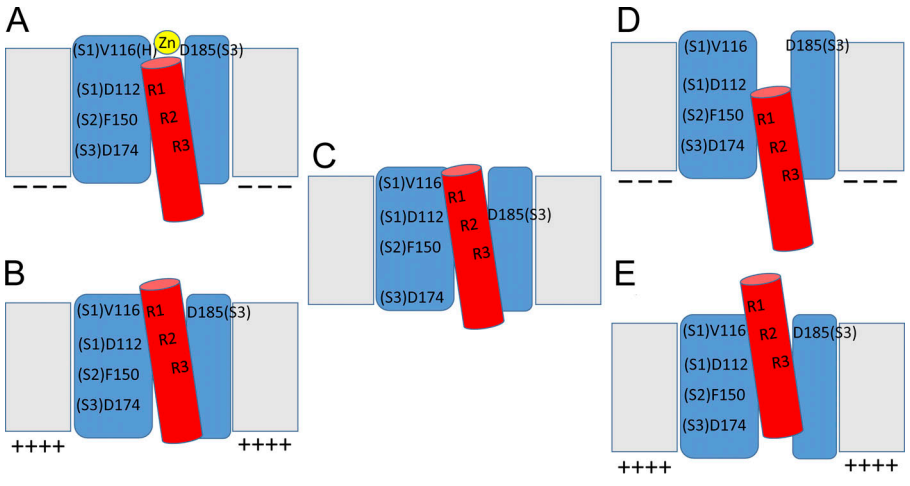

Figure 2. **Different models of voltage-gating in Hv1 channels. (A and B)** Simplified cartoon based on models of S4 movement in Hv1 channels from cryo-EM structures of the related VSP, EPR data on Hv1 (Li et al., 2014, 2015), and His accessibility (Kulleperuma et al., 2013). **(A)** Data by Cherny and coworkers in this issue suggest that a zinc ion (Zn) binds to V116H and D185 in the closed state at negative voltages. **(B)** Zinc has to unbind before outward S4 movement and channel opening at positive voltages. **(C)** Simplified cartoon of Hv1 channels based on the x-ray structure of the Hv1-VSP chimera (no voltage applied). The authors assumed this was a preactivated (nonconducting) state of Hv1 (Takeshita et al., 2014). **(D and E)** Simplified cartoon of models of S4 movement in Hv1 channels from cysteine accessibility studies (Gonzalez et al., 2010), leak currents generated in different mutants (Randolph et al., 2016), mutant cycle analysis (Berger and Isacoff, 2011; Chamberlin et al., 2014), and long MD simulations with applied transmembrane voltages (Geragotelis et al., 2020). S4 is shown in red and S1-S3 are shown in blue. Approximate locations of important residues in the different TM segments are shown, e.g., V116 in S1 as (S1)V116. Note that these cartoons are very simplified, and readers are encouraged to go to the original publications for more details about exact molecular arrangements.

chimera and VSP in different states (Li et al., 2014; Takeshita et al., 2014) and the plethora of experimental data and molecular simulations on Hv1 channels—there is no consensus about the molecular structures of these states. For example, how do we know that the x-ray structures of VSP (Li et al., 2014) and Hv1-VSP chimera (Takeshita et al., 2014) are equivalent to one of the structures of Hv1 in a native membrane? Which state—closed, preactivated, or open—is Hv1 in the x-ray structure (it is assumed to be in a preactivated closed state; Takeshita et al., 2014)? An open state is especially hard to identify by visual inspection of a proton channel structure or model: this is because one suggestion for proton conduction in Hv1 channel is that protons hop from one protonatable residue to another protonatable residue in a chain-like event across the protein (DeCoursey, 2013). Thus, protons do not necessarily need an aqueous pore to traverse a membrane protein. Mutagenesis studies have their own drawbacks: mutations can alter the protein conformation, cysteine accessibility is limited by the size of the cysteine reagents, and structural conclusions are often based on indirect evidence in mutagenesis studies.

Cherny and coworkers here propose that V116H and D185 are close together and coordinate Zn^{2+} in the closed state (Cherny et al., 2020). This is a different conformation than in the x-ray crystallography structure of Hv1-VSP (Takeshita et al., 2014), in which V116 and D185 are not close together (Fig. 2 C), but supports homology models of Hv1 based on, for example, the structures of VSP and EPR data from Hv1 (Fig. 2, A and B; Li et al., 2015). Cherny and coworkers further propose that, in response to depolarization, the first arginine in S4, R205 (R1), moves in between V116H and D185 (basically occupying the Zn^{2+} binding site) and therefore prevents Zn^{2+} binding to the open state (Fig. 2, A and B). Based on these two new constraints, the authors propose a model in which S4 moves "one click" in response to depolarization (Fig. 2, A and B). One click is defined as the three S4 charges (R1, R2, and R3), which are spaced three amino acids apart, moving outwards the distance of three amino acids, so that R2 takes the place of R1 and R3 takes the place of R2. However, this S4 movement would only generate around 1 e_0 of gating charge per subunit, which is contrary to previous experiments that have found that the gating charge is more around 3 e_0 per subunit in Hv1 channels (DeCoursey and Cherny, 1996; Gonzalez et al., 2010). To make the gating charge in their model larger, the authors refer to a mechanism that they proposed earlier (Cherny et al., 1995) that, in response to a depolarization, protons bind to protonatable groups (on the cytosolic side) and unbind from protonatable groups (on the extracellular side) on residues that are located inside the electrical field. This would also generate gating currents and add to the gating charge generated by S4 movement. However, another possibility is that the two states suggested here are a nonconducting, preactivated state and an open state, and that more deeply closed states of S4 exist. Data from other groups have been interpreted to suggest that the S4 movement in Hv1 channels is larger (2–3 clicks; Fig. 2, D and E; Berger and Isacoff, 2011; Chamberlin et al., 2014; Geragotelis et al., 2020; Randolph et al., 2016; Takeshita et al., 2014), which would be enough to generate the necessary gating charge. It is also possible that S4 moves further out in the open state than suggested here. The open state proposed here would place the second arginine R208 at the proposed selectivity filter residue D112 (Fig. 2 B), whereas other groups have suggested that the third arginine R211, instead of R208, is at the selectivity filter in the open state (Fig. 2 E; Berger and Isacoff, 2011; Chamberlin et al., 2014; Geragotelis et al., 2020; Randolph et al., 2016; Takeshita et al., 2014). The authors end by hedging their bets by concluding that the two states identified here are at least two states somewhere in the pathway between closed and open Hv1 channels. So, the final say about the structures of the closed and open states of Hv1 channels still seems to be something we have to wait for in a future study. However, the present work shows clearly that V116 and D185 are close enough in one of the closed states of Hv1 to coordinate Zn^{2+} and that outward S4 movement prevents Zn^{2+} binding.

Acknowledgments

Christopher J. Lingle served as editor.

The author's laboratory is funded by grants from the National Institutes of Health (R01 HL131461-01, R01 GM109762-06, and R01 GM139164).

The author declares no competing financial interests.

References

Berger, T.K., and E.Y. Isacoff. 2011. The pore of the voltage-gated proton channel. *Neuron.* 72:991–1000. https://doi.org/10.1016/j.neuron.2011.11.014

Chamberlin, A., F. Qiu, S. Rebolledo, Y. Wang, S.Y. Noskov, and H.P. Larsson. 2014. Hydrophobic plug functions as a gate in voltage-gated proton channels. *Proc. Natl. Acad. Sci. USA.* 111:E273–E282. https://doi.org/10.1073/pnas.1318018111

Cherny, V.V., V.S. Markin, and T.E. DeCoursey. 1995. The voltage-activated hydrogen ion conductance in rat alveolar epithelial cells is determined by the pH gradient. *J. Gen. Physiol.* 105:861–896. https://doi.org/10.1085/jgp.105.6.861

Cherny, V.V., B. Musset, D. Morgan, S. Thomas, S.M.E. Smith, and T.E. Decoursey. 2020. Engineered high-affinity zinc binding site reveals gating configurations of a human proton channel. *J. Gen. Physiol.* 152. 202012664.

De La Rosa, V., A.L. Bennett, and I.S. Ramsey. 2018. Coupling between an electrostatic network and the Zn^{2+} binding site modulates Hv1 activation. *J. Gen. Physiol.* 150:863–881. https://doi.org/10.1085/jgp.201711822

DeCoursey, T.E. 2013. Voltage-gated proton channels: molecular biology, physiology, and pathophysiology of the H(V) family. *Physiol. Rev.* 93:599–652. https://doi.org/10.1152/physrev.00011.2012

DeCoursey, T.E., and V.V. Cherny. 1996. Effects of buffer concentration on voltage-gated H+ currents: does diffusion limit the conductance? *Biophys. J.* 71:182–193. https://doi.org/10.1016/S0006-3495(96)79215-9

Geragotelis, A.D., M.L. Wood, H. Göddeke, L. Hong, P.D. Webster, E.K. Wong, J.A. Freites, F. Tombola, and D.J. Tobias. 2020. Voltage-dependent structural models of the human Hv1 proton channel from long-timescale molecular dynamics simulations. *Proc. Natl. Acad. Sci. USA.* 117:13490–13498. https://doi.org/10.1073/pnas.1920943117

Gonzalez, C., H.P. Koch, B.M. Drum, and H.P. Larsson. 2010. Strong cooperativity between subunits in voltage-gated proton channels. *Nat. Struct. Mol. Biol.* 17:51–56. https://doi.org/10.1038/nsmb.1739

Gonzalez, C., S. Rebolledo, M.E. Perez, and H.P. Larsson. 2013. Molecular mechanism of voltage sensing in voltage-gated proton channels. *J. Gen. Physiol.* 141:275–285. https://doi.org/10.1085/jgp.201210857

Koch, H.P., T. Kurokawa, Y. Okochi, M. Sasaki, Y. Okamura, and H.P. Larsson. 2008. Multimeric nature of voltage-gated proton channels. *Proc. Natl. Acad. Sci. USA.* 105:9111–9116. https://doi.org/10.1073/pnas.0801553105

Kulleperuma, K., S.M. Smith, D. Morgan, B. Musset, J. Holyoake, N. Chakrabarti, V.V. Cherny, T.E. DeCoursey, and R. Pomès. 2013. Construction and validation of a homology model of the human voltage-gated proton

channel hHV1. *J. Gen. Physiol.* 141:445–465. https://doi.org/10.1085/jgp.201210856

Lee, S.Y., J.A. Letts, and R. Mackinnon. 2008. Dimeric subunit stoichiometry of the human voltage-dependent proton channel Hv1. *Proc. Natl. Acad. Sci. USA.* 105:7692–7695. https://doi.org/10.1073/pnas.0803277105

Li, S.J., Q. Zhao, Q. Zhou, H. Unno, Y. Zhai, and F. Sun. 2010. The role and structure of the carboxyl-terminal domain of the human voltage-gated proton channel Hv1. *J. Biol. Chem.* 285:12047–12054. https://doi.org/10.1074/jbc.M109.040360

Li, Q., S. Wanderling, M. Paduch, D. Medovoy, A. Singharoy, R. McGreevy, C.A. Villalba-Galea, R.E. Hulse, B. Roux, K. Schulten, et al. 2014. Structural mechanism of voltage-dependent gating in an isolated voltage-sensing domain. *Nat. Struct. Mol. Biol.* 21:244–252. https://doi.org/10.1038/nsmb.2768

Li, Q., R. Shen, J.S. Treger, S.S. Wanderling, W. Milewski, K. Siwowska, F. Bezanilla, and E. Perozo. 2015. Resting state of the human proton channel dimer in a lipid bilayer. *Proc. Natl. Acad. Sci. USA.* 112:E5926–E5935. https://doi.org/10.1073/pnas.1515043112

Lishko, P.V., I.L. Botchkina, A. Fedorenko, and Y. Kirichok. 2010. Acid extrusion from human spermatozoa is mediated by flagellar voltage-gated proton channel. *Cell.* 140:327–337. https://doi.org/10.1016/j.cell.2009.12.053

Long, S.B., E.B. Campbell, and R. Mackinnon. 2005. Crystal structure of a mammalian voltage-dependent Shaker family K+ channel. *Science.* 309:897–903. https://doi.org/10.1126/science.1116269

Morgan, D., B. Musset, K. Kulleperuma, S.M. Smith, S. Rajan, V.V. Cherny, R. Pomès, and T.E. DeCoursey. 2013. Peregrination of the selectivity filter delineates the pore of the human voltage-gated proton channel hHV1. *J. Gen. Physiol.* 142:625–640. https://doi.org/10.1085/jgp.201311045

Qiu, F., A. Chamberlin, B.M. Watkins, A. Ionescu, M.E. Perez, R. Barro-Soria, C. González, S.Y. Noskov, and H.P. Larsson. 2016. Molecular mechanism of Zn2+ inhibition of a voltage-gated proton channel. *Proc. Natl. Acad. Sci. USA.* 113:E5962–E5971. https://doi.org/10.1073/pnas.1604082113

Ramsey, I.S., M.M. Moran, J.A. Chong, and D.E. Clapham. 2006. A voltage-gated proton-selective channel lacking the pore domain. *Nature.* 440:1213–1216. https://doi.org/10.1038/nature04700

Randolph, A.L., Y. Mokrab, A.L. Bennett, M.S. Sansom, and I.S. Ramsey. 2016. Proton currents constrain structural models of voltage sensor activation. *eLife.* 5. e18017. https://doi.org/10.7554/eLife.18017

Sasaki, M., M. Takagi, and Y. Okamura. 2006. A voltage sensor-domain protein is a voltage-gated proton channel. *Science.* 312:589–592. https://doi.org/10.1126/science.1122352

Takeshita, K., S. Sakata, E. Yamashita, Y. Fujiwara, A. Kawanabe, T. Kurokawa, Y. Okochi, M. Matsuda, H. Narita, Y. Okamura, et al. 2014. X-ray crystal structure of voltage-gated proton channel. *Nat. Struct. Mol. Biol.* 21:352–357. https://doi.org/10.1038/nsmb.2783

Tombola, F., M.H. Ulbrich, and E.Y. Isacoff. 2008. The voltage-gated proton channel Hv1 has two pores, each controlled by one voltage sensor. *Neuron.* 58:546–556. https://doi.org/10.1016/j.neuron.2008.03.026